Nanosecond Step-Scan FTIR Spectroscopy of Hemoglobin: Ligand Recombination and Protein Conformational Changes†

Xuehua Hu,‡ Heinz Frei,§ and Thomas G. Spiro*,‡

Department of Chemistry, Princeton University, Princeton, New Jersey 08544, and Structural Biology Division, Lawrence Berkeley National Laboratory, University of California, Berkeley, California 94720

Received June 24, 1996; Revised Manuscript Received August 21, 1996⊗

ABSTRACT: Step-scan FTIR spectroscopy with nanosecond time resolution is applied to the photocycle of carbonmonoxy hemoglobin (HbCO). The strong CO stretching band at 1951 cm^{-1} serves as a convenient monitor of the state of ligation. Both geminate and second-order phases of CO recombination occur at rates which are in excellent agreement with previous visible absorption measurements, showing the molecular mechanisms to be unperturbed by the high protein concentrations (6.7 mM in heme) required for adequate protein signals. While the extent of photolysis (43%) was insufficient to drive the R→T quaternary transition, the protein TRIR (time-resolved infrared) difference bands (1250−1700 cm^{-1}) nevertheless reveal interesting tertiary dynamics. Most of the bands are fully developed at very early times, possibly preceding the geminate recombination phase ($\tau = 50$ ns). Some bands arise more slowly, however, with a time constant of 0.4 μs, reflecting a tertiary motion which is coincident with a quaternary motion previously detected by ultraviolet resonance Raman spectroscopy of fully photolyzed HbCO. Relaxation of the TRIR bands is either faster ($\tau = \sim 90$ μs) or slower ($\tau = \sim 250$ μs) than CO rebinding (effective time constant of 160 μs), suggesting either a distribution of tertiary processes or a chain inequivalence in CO rebinding.

We report the first application of time-resolved FTIR spectroscopy (Uhmann et al., 1991; Weidlich & Siebert, 1993; Plunkett et al., 1995; Hage et al., 1996) to the evolution of protein structure in hemoglobin on the nanosecond to millisecond time scale. Interest in this problem centers on the issue of allostery, for which Hb is a paradigm (Perutz, 1990). The tetrameric protein attains two limiting structures, R and T (Baldwin & Chothia, 1979), which are associated with high- and low-affinity states. R is favored when all four subunits are ligated, while T is favored when they are unligated; the switch between them at an intermediate stage of ligation accounts for the main features of cooperativity in ligand binding (Monod et al., 1965; Hopfield et al., 1971; Ackers et al., 1992). But what are the molecular motions that lead from one structure to another, and what are their time scales? In a more general context, what do motions in Hb tell us about protein dynamics?

New structure-sensitive experimental probes have become available which promise fresh insights into these questions. Time-resolved ultraviolet resonance Raman (UVRR) spectroscopy has recently been applied to the allosteric reaction coordinate in Hb (Jayaraman et al., 1995). This technique monitors vibrational signatures of aromatic residues, which provide *in-situ* probes of protein structure change. The UVRR data provided the first determination of the time scales for inter-helix motions and for the formation of inter-subunit contacts. UVRR spectroscopy is limited, however, by the availability of UV-absorbing chromophores. Infrared spectroscopy, on the other hand, responds to all molecular vibrations, in proportion to the associated change in dipole moment. Of course, this generality comes at the price of low selectivity and sensitivity. However, the advent of high-precision Fourier transform (FTIR) hardware and software permits the acquisition of difference signals down to the level of single residues in proteins (Gerwert, 1989; Engelhard et al., 1985; Mäntele, 1993). Consequently, structure *changes* can be detected with high sensitivity. This capability has generated intense interest in applying FTIR techniques in a time-resolved mode, and rapid technical advances now make this possible on time scales down to nanoseconds (Weidlich & Siebert, 1993; Hartland et al., 1992; Braiman & Rothschild, 1988; Hage et al., 1996). Even faster transients can be detected with single-wavelength pulsed laser techniques, which are also being applied to proteins (Chernoff et al., 1980; Anfinrud et al., 1989; Stoutland et al., 1992; Causgrove & Dyer, 1996).

In this first nanosecond FTIR study of Hb, [microsecond IR studies had recently appeared (Causgrove & Dyer, 1993; Plunkett et al., 1995)], we apply well-established methodology for transient generation of deligated protein by photolysis of the CO adduct. The experiment did not monitor the R−T reaction coordinate because the photolysis levels were insufficient to induce conversion to the T state. Nevertheless interesting and complex tertiary structure dynamics are revealed.

MATERIALS AND METHODS

Sample Preparation. Adult human hemoglobin (HbA) was purified from fresh human blood following standard procedures (Antonini & Brunori, 1971). The red cells were

† This work was supported by NIH Grant GM 25158 (T.G.S) and by the Director, Office of Energy Research, Office of Basic Energy Sciences, Chemical Sciences Division, of the U.S. Department of Energy under Contract No. DE-AC03-76SF00098 (H.F.).

* Author to whom correspondence should be addressed.
‡ Princeton University.
§ University of California.

⊗ Abstract published in *Advance ACS Abstracts,* October 1, 1996.

S0006-2960(96)01522-X CCC: $12.00

exposed to CO, separated by centrifugation in saline solution (9 g/L), and subsequently ruptured by dilution in distilled water. After centrifugation to separate the membrane fragments, HbCO supernatant was stripped of organic phosphates by ion-exchange chromatography. The concentrated samples were diluted in D_2O buffer saturated with CO gas and then reconcentrated using Amico centrifugal concentrator. This procedure was repeated several times until exchange of H_2O by D_2O was estimated to be greater than 98% by the IR absorption of water at 3400 cm^{-1}. The protein was left in the D_2O buffer for at least 36 h to secure complete exchange of labile protons. The final Hb concentration was 6.7 mM (in heme) in 50 mM phosphate buffer at pD 7.4 saturated with 1 atm of CO gas.

Spectral Measurements. The step-scan FTIR instrument was described elsewhere [Hage et al., 1996; for a general description of the step-scan FTIR set-up, see Figure 2 in Uhmann et al. (1991)]. Briefly, a Bruker IFS 88 FTIR spectrometer with step-scan option was used. For nanosecond time-resolved measurements, a 50 MHz photovoltaic MCT detector with a built-in low-noise preamplifier was employed. This preamplifier provides two outputs: a DC output furnishing the static interferogram and an AC output furnishing the laser-induced change of the interferogram. The AC-coupled signal was amplified by a factor of 200 by another amplifier (500 MHz), in order to make use of the full dynamic range of an 8 bit digitizer (200 MHz). Both AC- and DC-coupled signals were then simultaneously sampled, and Fourier transformation of the AC-coupled interferogram uses the phase obtained from the DC-coupled interferogram.

The time response of the system was ~20 ns, as determined via the scattered 1064 nm radiation of the 9 ns laser pulse of a Nd:YAG laser. Transient difference FTIR spectra from −60 to 940 ns were recorded at 10 ns intervals. One-sided interferograms with 1141 mirror positions were collected to obtain 4 cm^{-1} spectral resolution with spectral window of 2050−850 cm^{-1}. At each mirror position 30 signals were averaged in order to increase the signal/noise ratio, resulting in a total data collection time of ~1 h per experiment. Data from five successive 1-h scans were averaged for further signal/noise improvement.

The second harmonic emission (532 nm) of a Q-switched Nd:YAG laser (9 ns pulse width, 10 Hz) was used as the pump laser. The laser power was typically 7 mJ/pulse focused to a ~7 mm spot. The temperature of the sample was kept at 22 ± 1 °C during the experiments. Heating effects are minimal because of good thermal conduction to the windows of the IR cell; no protein depletion was detected even after 6 h of irradiation. CaF_2 windows were used to give unobstructed access to the spectral window above 1200 cm^{-1}; their transparency in the visible region also permitted the acquisition of visible absorption spectra of the loaded FTIR cell to check the sample integrity. In order to keep the IR absorption of the most intense band below 0.9, 15 μm spacers were used, ensuring that the IR detector operates within its linear region.

The microsecond time-resolved measurements were performed similarly. A 200 kHz 16 bit digitizer was used and a DC-coupled step-scan run was conducted first without excitation of the sample. The phase was stored and then used for the Fourier transformation of the AC-coupled interferograms. The transient difference FTIR spectra from 5 μs to 1 ms were recorded at 5 μs intervals. Difference spectra (ΔA) were calculated as previously described (Uhmann et al., 1991).

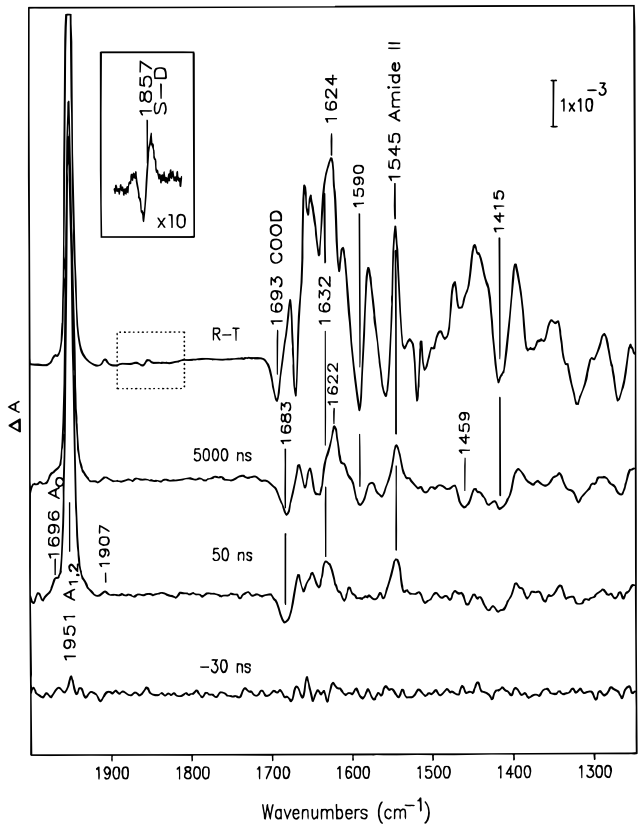

FIGURE 1: TRIR difference spectra (HbCO minus photoproduct, pD 7.4) at the indicated time delays between the photolysis pulse and spectral acquisition. The −30 ns trace is a control, showing the level of noise. The "5000" ns spectrum is the actual spectrum with 5 μs delay, but the 50 ns spectrum is the result of co-adding the first ten 10 ns time slices, in order to improve signal/noise. Shown for comparison is the static difference spectrum of HbCO minus deoxyHb [labeled R−T; see Gregoriou et al. (1995) for experimental details], scaled to the amplitude of the TRIR ν_{CO} band at time zero. The intense CO stretching band (1951 and 1969 cm^{-1} for $A_{1,2}$ and A_0 substates; 1907 cm^{-1} for ^{13}CO satellite) monitors the level of CO binding, while the bands below 1700 cm^{-1} arise from vibrations of the protein. The S−D band (1857 cm^{-1}) is expanded 10-fold in the inset.

Since the measured time response of the instrument was about 20 ns, pairs of 10 ns time slices were co-added and taken as single data points for kinetic analysis of the CO stretching bands in the nanosecond regime. The lower signal strength of the protein bands required ten 10-ns time slices to be co-added. The first six slices (from −60 to 0 ns) were co-added and taken as the −30 ns time-resolved infrared (TRIR) spectrum. In the microsecond time regime, however, no co-addition was necessary.

RESULTS AND DISCUSSION

Overview of the Time-Resolved Spectra. The TRIR difference spectra (HbCO minus the photoproduct) show strong CO stretching bands at 1951 cm^{-1} and a series of protein-associated bands below 1700 cm^{-1} (Figure 1). The spectral quality is high enough to permit detection of the satellite ^{13}CO stretching band (1907 cm^{-1}, 1.08% natural abundance) as well as the small amount of the A_0 substate (1969 cm^{-1}; Ormos et al., 1988; Potter et al., 1990) present at neutral pH.

The protein bands bear some resemblance to those seen in the static HbCO minus deoxy Hb FTIR spectrum (Figure

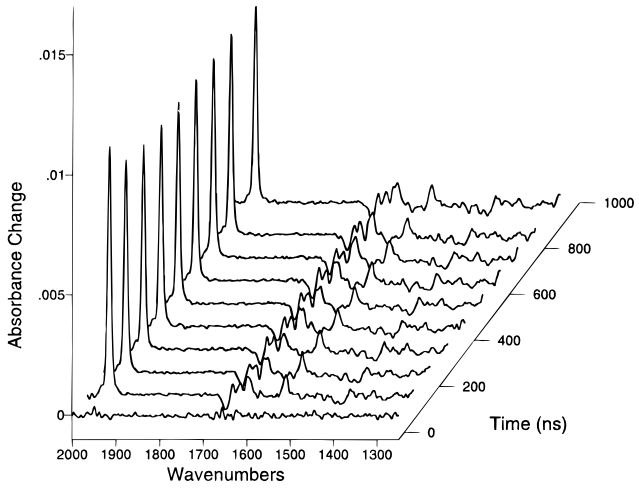

FIGURE 2: Progress of the TRIR difference spectra over the first microsecond after photolysis at the following delays: −30, 50, 150, 250, 350, 450, 550, 650, 750, and 890 ns. Each spectrum (except −30 ns) was obtained by co-adding ten 10 ns time slices.

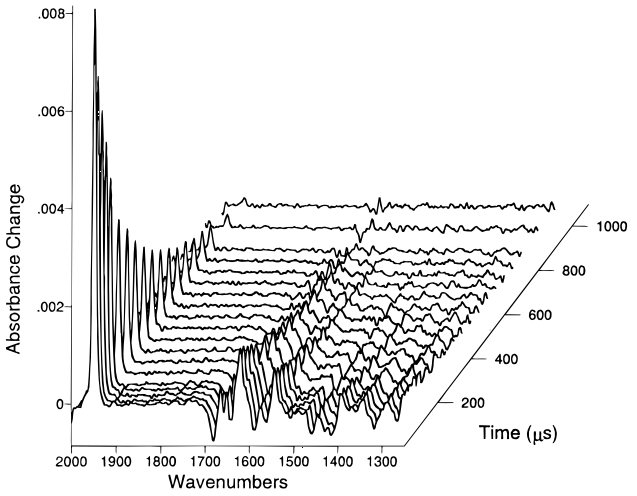

FIGURE 3: Progress of the TRIR difference spectra over the first millisecond after photolysis at the following delays: 5, 25, 50, 100, 150, 200, 250, 300, 350, 400, 450, 500, 550, 600, 650, 600, 800, and 900 μs. The absorbance scale is expanded relative to Figure 2, in order to show the decays more clearly.

1, top), but there are also distinct differences. These differences reveal features unique to the T state (deoxyHb), inasmuch as the extent of photolysis in this study is too low to permit the photoproduct to evolve to the T state (43%, see below). The absence of a well-resolved bisignate band at 1857 cm^{-1} (see inset, Figure 1) in the TRIR spectra confirms the absence of T state molecules. This band results from a shift in the S−D stretching frequency of Cys α104 and represents an important monitor of quaternary structure (Alben & Bare, 1980; Gregoriou et al., 1995). Of particular note are the absence of a negative band at 1693 cm^{-1} in the transient difference spectra and the presence of a band at 1683 cm^{-1}. The negative 1693 cm^{-1} band in the R−T difference spectrum has been tentatively assigned (Gregoriou et al., 1995) to the C═O stretch of the Asp β99 carboxylate group upon protonation in the T state. This band was found to be missing in the T state of Hb Kempsey, a mutant in which Asp β99 is replace by Asn. Its absence in the TRIR spectra is consistent with the expected absence of Asp β99 protonation in photolyzed R state molecules. The 1683 cm^{-1} TRIR band might be due to the C═O (amide I) vibration of a primary amide side chain, of Asn or Gln. The frequency is higher than expected for backbone amide bonds in Hb (Byler & Susi, 1986). The Hb Kempsey R−T difference spectrum (Gregoriou et al., 1995) contained a negative 1680 cm^{-1} band, which was suggested to arise from H-bond changes in the Asn β99 side chain upon conversion to the T state. It is possible that a different Asn or a Gln side chain undergoes a change in its environment when the CO is photolyzed, accounting for the 1683 cm^{-1} TRIR band. As will be seen, this band relaxes with a faster rate than most of the other protein bands. These other bands are at frequencies corresponding to various main chain and side chain vibrations of the protein (Gregoriou, 1995), but because of the spectral congestion, assignments are purely conjectural at this stage.

All of the protein bands in the 50 ns TRIR spectrum are still present at 5 μs (Figure 1), but there are additional bands (e.g., 1622, 1590, 1459 cm^{-1}) in the longer time spectrum, showing that there is evolution of the protein structure on the microsecond time scale. The time course of the TRIR spectra is shown in Figures 2 and 3 (note the 2-fold ordinate scale expansion in Figure 3). It is apparent that the CO peak initially decreases to an amplitude that remains nearly

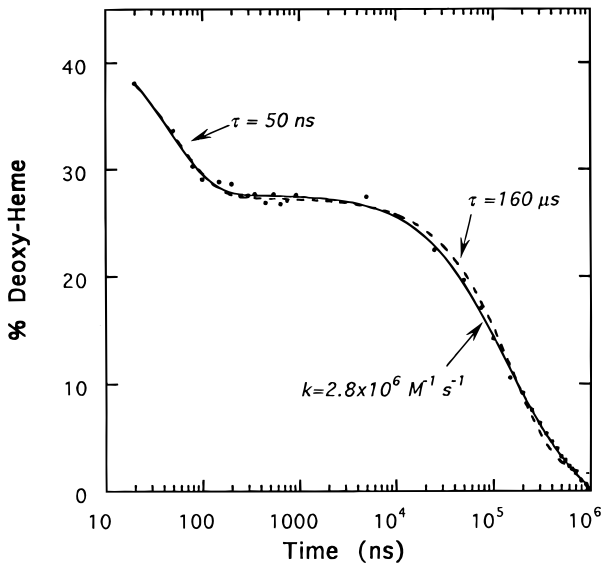

FIGURE 4: Kinetics of recombination of CO to photolyzed HbCO obtained from quantitation of the bound CO stretching band amplitude. The *y*-axis is the fraction of deoxy-heme in the sample (6.7 mM). The dotted line is a bi-exponential fit to the data, with time constants τ = 50 (±5) ns and τ = 160 (±10) μs. The solid line is a fit using the single-exponential equation $y = a + b\exp(-k_{gem}t)$ for the rapid phase with $a = 0.27$, $b = 0.16$, and $\tau_{gem} = 1/k_{gem} = 50$ (±5) ns. The photolysis yield is calculated as $a + b = 43\%$, and the geminate rebinding yield is $\phi = b/(a + b) = 37\%$. For the slow phase the solid line is a fit using the second-order equation $y = C_{CO}/\{[1 + C_{CO}/a_0]\exp(-C_{CO}k_{2nd}t) - 1\}/6.7$ mM, with $a_0 = 6.7a = 1.84$ mM. The value of k_{2nd} is 2.8 (±0.2) × 10^6 M^{-1} s^{-1}, and the free CO concentration before photolysis is $C_{CO} = 0.91$ (±0.15) mM (in agreement with the solubility at 1 atm pressure).

constant over the first microsecond and then decays in the course of the first millisecond. The protein peaks decay on the same time scale (albeit at different rates, see below), as the Hb is returned to HbCO, the starting point of the photocycle.

CO Recombination Kinetics. The concentration of heme-bound CO is readily quantitated by normalizing the CO stretching peak to that of HbCO. The time course of this concentration is plotted in Figure 4 as the fraction of deoxy-heme in the sample. The initial relaxation is accurately fit by a single exponential with a time constant of 50 ns (Table

Table 1: Kinetic Constants (τ, in μs) from TRIR[a]

geminate rebinding	0.05 ± 0.005[b]
1590 cm^{-1} growth	0.4 ± 0.2[c]
1683 cm^{-1} decay	90 ± 10
second-order rebinding	$\sim 160 \pm 10$[d]
1622 cm^{-1} decay	250 ± 20
1590 cm^{-1} decay	220 ± 20
1545 cm^{-1} decay	240 ± 20
1459 cm^{-1} decay	270 ± 20
1415 cm^{-1} decay	280 ± 30

[a] The uncertainty is the standard deviation from the data fitting. [b] Compare 0.044 from Hofrichter et al. (1983). [c] Compare 0.91 for tertiary transient from Hofrichter et al. (1983). [d] Best exponential decay fit; the second order rate constant is $(2.8 \pm 0.2) \times 10^6$ M^{-1} s^{-1}.

1). This value is in excellent agreement with that obtained by Hofrichter et al. (1983), who analyzed the time evolution of the heme absorption spectrum. It is also within experimental error (~20 ns time resolution in each experiment) of the 20 ns value obtained by fitting time-resolved visible and UV resonance Raman spectra (Jayaraman et al. 1995). Using the exponential dependence, we calculate the initial degree of photolysis to be 43%, from the heme-CO concentration at zero time.

This first relaxation is the geminate phase of the CO recombination (the recombining CO molecules have not left the protein, and the rate is independent of CO concentration; Hofrichter et al., 1983). The geminate yield as determined from the plateau in Figure 4 is 37%. This is somewhat lower than the ~50% geminate yield obtained under conditions of 100% photolysis (Hofrichter et al., 1983; Jayaraman et al., 1995; Scott & Friedman, 1984), but it cannot be excluded that this modest difference might be due to non-constancy of the IR absorptivity, i.e., geminately rebound CO might have a lower absorptivity, because of alterations in the protein environment, than does CO in the HbCO ground state.

Assuming the 37% value to be correct, only 27% of the heme groups remain unligated at the end of the geminate phase. This means that each Hb tetramer contains one deoxy-heme, on average. Since two or more deoxy-hemes are required for the protein to switch to the T state (Baldwin, 1975; Ackers et al., 1992), it is clear that most of the molecules do not undergo this conversion and that the TRIR spectra represent mostly R state tetramers.

The second phase of the relaxation is on the millisecond time scale, and reflects second order recombination of CO molecules from outside the protein. The rate is known to depend on the CO concentration (Hofrichter et al., 1983; Sawicki & Gibson, 1976), and it can be seen in Figure 4 that the best fit to an exponential ($\tau = 160$ μs) deviates systematically from the data. The deviations reflect the fact that because of the high heme concentration (6.7 mM), and the low CO solubility (~1 mM at 1 atm pressure), the reaction conditions are not first order. An excellent fit is obtained for a second-order reaction, with a rate constant of 2.8×10^6 M^{-1} s^{-1}. This value is in good agreement with the value 6×10^6 M^{-1} s^{-1} obtained by Hofrichter et al. (1983) under conditions of low photolysis (22%), and it is in the range expected for R state Hb (DeYoung et al., 1976; Sawicki & Gibson, 1976).

These results are important in showing that the TRIR technique gives clean kinetics which are in quantitative agreement with other methods, despite the much higher protein concentration required for FTIR spectroscopy. Good second-order kinetics have also been reported from TRIR measurements on MbCO (Mb = myoglobin) (Causgrove & Dyer, 1993; Plunkett et al., 1995).

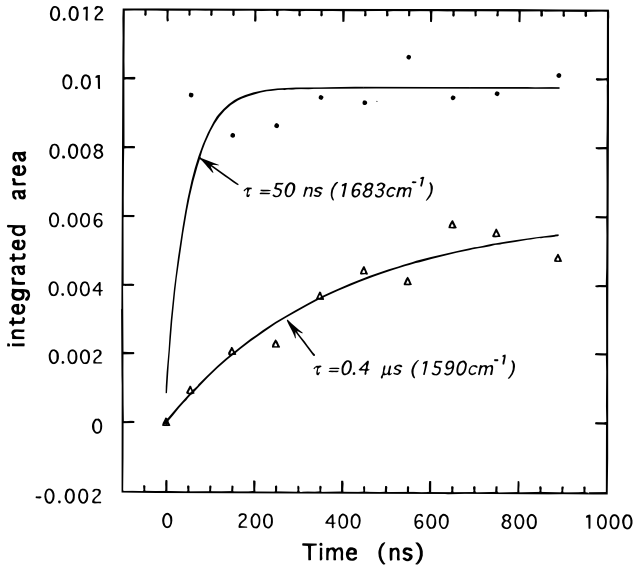

FIGURE 5: Growth of the indicated TRIR bands in the nanosecond regime. The solid lines are exponential fits with the indicated time constants. For the 1683 cm^{-1} band (and most of the other protein bands) the rise time may be faster than 50 ns.

Kinetics of Protein Conformational Changes. When the protein TRIR bands are examined, most of them are present in the earliest spectra, but some evolve more slowly. For example, the 1590 cm^{-1} negative band is not present in the 50 ns spectrum (Figure 1), but grows in with a time constant of 0.4 μs (Figure 5). This value is not far from the 0.9 μs optical transient observed by Hofrichter et al. (1983), and attributed by them to a tertiary conformation change. It is also coincident with the 0.5 μs UVRR transient (Jayaraman et al., 1995), which was assigned to an intermediate (S) in the R→T pathway. This transient was suggested to arise from rotation of the subunits to their T state positions, since the UVRR spectrum of S showed all the signals, albeit attenuated, that are associated with the T state contacts. Likewise the circular dichroism spectrum of this intermediate has recently been reported to resemble that of the T state (Björling et al, 1996). The simplest interpretation of these data is that CO photodissociation leads to a submicrosecond tertiary change, which impels the quaternary rearrangement in those tetramers that are committed to this process by virtue of the number of deoxy-hemes.

In contrast to the 1590 cm^{-1} band, the intensity of the 1683 cm^{-1} band (Figure 5), and of most of the other TRIR bands, is essentially fully developed in the earliest spectra. The data are not accurate enough to establish whether this development precedes the 50 ns geminate recombination process (see Figure 5). The first UVRR-detectable protein structure change (Jayaraman et al., 1995) was found to be coincident with geminate recombination (and with escape of the remaining CO molecules from the heme pocket), and the TRIR bands may be responding to this process. It is likely, however, that earlier events also contribute to the TRIR difference spectra; induced IR absorptions in the amide I regime with 6−8 ps rise time have been found in Mb (Causgrove & Dyer, 1996). The present data include spectral scans with 10 ns time intervals, but the signal/noise required co-adding ten intervals in order to be confident about the protein peaks. It will be an important objective of future work to improve the early time signal quality in order to

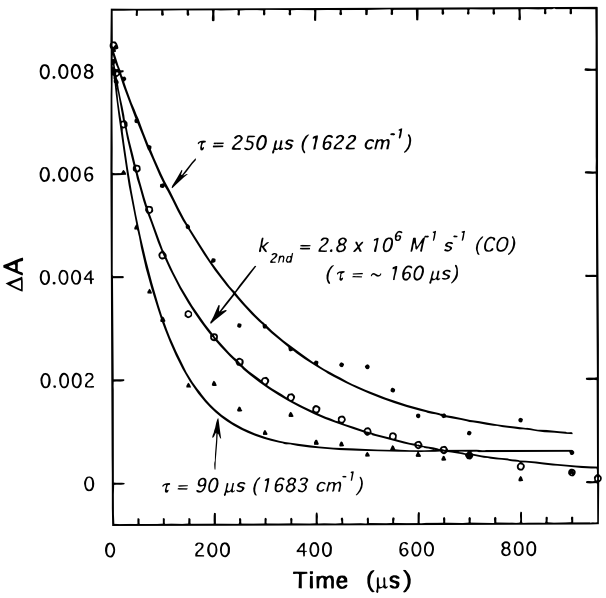

FIGURE 6: Decay of the TRIR bands at 1683 and 1622 cm^{-1} in the microsecond regime compared with CO rebinding. The latter is a fit of a second-order reaction with the indicated rate constant. The 1683 and 1622 cm^{-1} band amplitudes are scaled up by factors of 10.7 and 6.9 to facilitate comparison with single exponential fits. Decay is faster than CO rebinding for the 1683 cm^{-1} band but slower for the 1622 cm^{-1} and other protein bands (not shown, see Table 1).

determine which spectral features precede the geminate phase.

When the longer time data are examined (Figure 6), two classes of behavior are observed for the relaxation of the protein peaks. The 1683 cm^{-1} band relaxes with a time constant of 90 μs, while most of the bands relax with time constants near 250 μs (Table 1). As expected, there is no relaxation at ~20 μs, the time constant for the final evolution of the T state in fully photolyzed samples (Hofrichter et el., 1983; Jayaraman et al., 1995). As can be seen in Figure 6 and Table 1, the CO recombination rate (effective time constant of 160 μs) lies between the two classes of protein relaxation. There are two alternate explanations for this behavior: (1) there are protein tertiary structure changes which precede as well as follow the recombination event, or (2) the two protein relaxations reflect different recombination rates for α and β chains within the tetramer, while the FeC−O band relaxation represents an average of the two rates. Further experiments are required to distinguish these possibilities.

CONCLUSIONS

This study establishes that time-resolved FTIR spectroscopy is capable of monitoring protein structure change as well as ligand recombination on time scales down to tens of nanoseconds. Both geminate and second-order recombination of CO to Hb are determined with excellent reliability, showing that the high protein concentrations required for adequate protein signals do not perturb the molecular mechanisms. Although the level of photolysis was below that necessary to drive the R→T transition, the data reveal several dynamical processes in the protein. Much of the TRIR spectrum is established very early, possibly preceding the geminate recombination phase, and relaxes heterogeneously, reflecting either a distribution of tertiary processes or chain inequivalence in CO rebinding. Intermediate phases of protein structure change are also detected via selected protein bands. One of these (τ = 0.4 μs) signals a tertiary change that may also be involved in the quaternary rearrangement of fully photolyzed molecules. By simultaneously monitoring many parts of the protein as well as the ligation state of the heme, the TRIR spectra reveal a rich array of protein dynamics in Hb.

ACKNOWLEDGMENT

We thank Drs. Richard Palmer, Thomas Tague, and Brain Dyer for helpful discussions.

REFERENCES

Ackers, G. K., Doyle, M. L., Myers, D., & Daugherty, M. A. (1992) *Science* 255, 54.
Alben, J. O., & Bare, G. H. (1980) *J. Biol. Chem. 255*, 3892.
Anfinrud, P. A., Han, C., & Hochstrasser, R. M. (1989) *Proc. Natl. Acad. Sci. U.S.A. 86*, 8387.
Antonini, E., & Brunori, M. (1971) in *Hemoglobin and Myoglobin and their Reactions with Ligands* (Neuberger, A., & Tatum, E. L., Eds.) pp 2−4, Elsevier, New York.
Baldwin, J. (1975) *Prog. Biophys. Mol. Biol. 29*, 225.
Baldwin, J., & Chothia, C. (1979) *J. Mol. Biol. 29*, 175.
Björling, S. C., Goldbeck, R. A., Paquette, S. J., Milder, S. J., & Kliger, D. S. (1996) *Biochemistry 35*, 8619.
Braiman, M. S., & Rothschild, K. J. (1988) *Annu. Rev. Biophys. Biophys. Chem. 17*, 541.
Byler, D. M., & Susi, H. (1986) *Biopolymers 25*, 469.
Causgrove, T. P., & Dyer, R. B. (1993) *Biochemistry 32*, 11985.
Causgrove, T. P., & Dyer, R. B. (1996) *J. Phys. Chem. 100*, 3273.
Chernoff, D. A., Hochstrasser, R. M., & Steele, A. W. (1980) *Proc. Natl. Acad. Sci. U.S.A. 77*, 5606.
DeYoung, A., Pennelly, R. R., Tan-Wilson, A. L., & Nobel, R. W. (1976) *J. Biol. Chem. 251*, 6692.
Engelhard, M., Gerwert, K., Hess, B., Kreutz, W., & Siebert, F. (1985) *Biochemistry 24*, 400.
Gerwert, K., Hess, B., Soppa, J., & Oesterhelt, D. (1989) *Proc. Natl. Acad. Sci. U.S.A. 86*, 4943.
Gregoriou, V. G., Jayaraman, V., Hu, X., & Spiro, T. G. (1995) *Biochemistry 34*, 6876.
Hage, W., Kim, M., Frei, H., & Mathies, R. A. (1996) *J. Phys. Chem.* (in press).
Hartland, G. B., Xie, W., Dai, H. L., Simon, A., & Anderson, M. J. (1992) *Rev. Sci. Instrum. 63*, 3261.
Hofrichter, J., Sommer, J. H., Henry, E. R., & Eaton, W. A. (1983) *Proc. Natl. Acad. Sci. U.S.A. 80*, 2235.
Jayaraman, V., Rodgers, K. R., Mukerji, I., & Spiro, T. G. (1995) *Science 269*, 1843.
Hopfield, J. J., Shulman, R. G., & Ogawa, S. (1971) *J. Mol. Biol. 61*, 425.
Mäntele, W. (1993) *Trends Biochem. Sci. 18*, 197.
Monod, J. L., Wyman, J., & Changeux, J. P. (1965) *J. Mol. Biol. 12*, 88.
Plunkett, S. E., Chao, J. L., Tague, T. J., & Palmer, R. A. (1995) *Appl. Spectrosc. 49*, 702.
Potter, W. T., Hazzard, J. H., Choc, M. G., Tucker, M. P., & Caughey, W. S. (1990) *Biochemistry 29*, 6283.
Ormos, P., Braunstein, D., Fraunfelder, H., Hong, M. K., Lin, S. L., Sauke, T. D., & Young, R. D. (1988) *Proc. Natl. Acad. Sci. U.S.A.* 85, 8492.
Perutz, M. F. (1990) *Annu. Rev. Physiol.* 52, 1.
Sawicki, C., & Gibson, Q. H. (1976) *J. Biol. Chem. 251*, 1533.
Scott, T. W., & Friedman, J. M. (1984) *J. Am. Chem. Soc. 106*, 5677.
Stoutland, P. O., Dyer, R. B., & Woodruff, W. H. (1992) *Science 257*. 1913.
Uhmann, W., Becker, A., Taran, C., & Siebert, F. (1991) *Appl. Spectrosc. 45*, 390.
Weidlich, O., & Siebert, F. (1993) *Appl. Spectrosc. 47*, 1394.

BI961522N